



AIAA-2002-0381

**Computing Aerodynamic Performance
of a 2D Iced Airfoil:
Blocking Topology and Grid Generation**

X. Chi, B. Zhu, and T. I-P. Shih
Michigan State University
East Lansing, Michigan

J.W. Slater, H.E. Addy, and Y.K. Choo
NASA – Glenn Research Center
Cleveland, Ohio

This is a preprint or reprint of a paper intended for presentation at a conference. Because changes may be made before formal publication, this is made available with the understanding that it will not be cited or reproduced without the permission of the author.

40th Aerospace Sciences Meeting & Exhibit

**14–17 January 2002
Reno, Nevada**

Computing Aerodynamic Performance of a 2D Iced Airfoil: Blocking Topology and Grid Generation

X. Chi,^{*} B. Zhu,^{**} and T. I-P. Shih[#]

Department of Mechanical Engineering, Michigan State University
East Lansing, Michigan 48824-1226

J.W. Slater⁺, H.E. Addy⁺, and Y.K. Choo⁺

NASA – Glenn Research Center
Cleveland, Ohio 44135

ABSTRACT

The ice accrued on airfoils can have enormously complicated shapes with multiple protruded horns and feathers. In this paper, several blocking topologies are proposed and evaluated on their ability to produce high-quality structured multi-block grid systems. A transition-layer grid is introduced to ensure that jaggedness on the ice-surface geometry do not to propagate into the domain. This is important for grid-generation methods based on hyperbolic PDEs and algebraic transfinite interpolation. A “thick” wrap-around grid is introduced to ensure that grid lines clustered next to solid walls do not propagate as streaks of tightly packed grid lines into the interior of the domain along block boundaries. For ice shapes that are not too complicated, a method is presented for generating high-quality single-block grids.

To demonstrate the usefulness of the methods developed, grids and CFD solutions were generated for two iced airfoils: the NLF0414 airfoil with and without the 623-ice shape and the B575/767 airfoil with and without the 145m-ice shape. To validate the computations,

the computed lift coefficients as a function of angle of attack were compared with available experimental data.

The ice shapes and the blocking topologies were prepared by NASA Glenn’s SmagIce software. The grid systems were generated by using a four-boundary method based on Hermite interpolation with controls on clustering, orthogonality next to walls, and C^1 continuity across block boundaries. The flow was modeled by the ensemble-averaged compressible Navier-Stokes equations, closed by the shear-stress transport turbulence model in which the integration is to the wall. All solutions were generated by using the NPARC WIND code.

INTRODUCTION

When an aircraft flies into environmental conditions where ice can form on its airfoils, catastrophic effects on the aircraft’s aerodynamics can occur. When compared to a “clean” airfoil (i.e., an airfoil without accrued ice), an “iced” airfoil can have not only reduced lift, but also stall occurring at markedly lower angles of attack.¹ This is because the ice buildup is mostly about the airfoil’s leading edge, whose geometry is critical in determining lift and stall.

The icing problem has two components. One is ice accretion, and the other is icing effect. Ice accretion is concerned with how ice forms on the airfoil surface and its evolving shape as a function of Mach number, angle of attack, airfoil shape, airfoil size, environmental parameters, and duration under favorable conditions for ice accretion. Icing effects are concerned with the aerodynamic performance of an airfoil that has ice of different sizes and shapes formed on it.

This study addresses issues related to computational fluid dynamics (CFD) simulations of icing effects. Icing

^{*} Graduate Student.

^{**} Research Associate.

[#] Professor. Associate Fellow AIAA.

⁺ Aerospace Engineer, Inlet Branch. Member AIAA.

⁺⁺ Aerospace Engineer, Icing Branch. Member AIAA.

effects can be studied by flight tests, wind-tunnel tests, and CFD simulations. Flight tests are the most realistic but expensive. Tests in wind tunnels offer the advantage of a controlled environment, but there are problems in reproducing actual flight conditions and scaling certain geometric and operating parameters. CFD offers the advantage of low cost and the ability to simulate realistic conditions. However, the accuracy of CFD hinges on the quality of the grid system in resolving the geometry and the flow and the "appropriateness" of the turbulence model in capturing the relevant physics.

In order to generate a grid, one must first obtain the ice-surface geometry. Currently, methods exist that can be used to measure ice surfaces on airfoils in two-dimensional (2D) cross sections, which involve meticulous tracing with subsequent digitization. Methods for measuring three-dimensional (3D) ice surfaces, however, are still being developed. Traditional optical scanning methods for 3D surfaces are not useful because ice is transparent. Though a transparent surface can be made opaque by covering it with a paint or powder, it is extremely difficult to cover a material that can melt with a thin layer that is of the same thickness everywhere. As a result, reliable data of ice shapes on airfoils are mostly 2D.

With limited information on 3D ice surfaces, there are very few 3D simulations of iced airfoils. When 3D simulations are performed, the interest is on the qualitative features of the flow with focus on 3D effects.² So far, simulations that focus on iced airfoil's aerodynamic performance have assumed the flow to be 2D and steady. The generation of a performance curve, such as lift as a function of angle of attack, requires many simulations, which render 3D simulations prohibitively expensive and time consuming even if 3D ice-surface geometries can be measured reliably. The assumption of steady flow is reasonable except near stall, when the flow can become unsteady.

2D simulations that study how ice shapes affect airfoil performance have been reported by a number of investigators.²⁻⁴ Several different types of ice shapes have been studied. Validity of these studies was assessed by comparing computed results with measurements from wind-tunnel tests. Results obtained show that reasonable results can be obtained for cases in which the ice shapes do not protrude too much. But, if there are significant features such as large horns and feathers, then the predictions can be significantly different from the measurements. There are several reasons for the poor agreement when the ice shape involves large horns and feathers. One reason is that high-quality grid systems become much harder to generate.

The objective of this study is to propose and evaluate methods that enable the generation of high-quality structured grid systems for 2D iced airfoils with highly complicated ice shapes, including multiple horns that protrude extensively.

GRID GENERATION ISSUES

The grid system used in a CFD simulation must resolve the geometry and enable the governing equations with the turbulence model to resolve all of the relevant physics with minimum grid-induced errors. For airfoils with ice formed on it, this is a challenging task. From what NASA has learned from previous studies,²⁻⁴ structured-grid approach should serve as a good reference or baseline, against which other grid approaches can be compared and assessed. If structured grids are to be used, then there are two main issues.

The first main issue is *surface preparation*. This issue arises because the geometry of iced airfoils is complicated not just with protruded horns and feathers, but also with small-scale surface roughness. One system that has been used to prepare ice-surface geometry with various levels of smoothing is NASA's Turbo-GRD code.^{5,6} A comprehensive system currently being developed and maintained at NASA Glenn is SmagIce⁷. SmagIce 1.0 is a software tool kit that provides interactive ice surface preparation for grid generation and ice shape characterization. In this study, SmagIce 1.0 was used to prepare the ice shapes through its smoothing routines. SmagIce was also used in generating the block topologies.

The second main issue is *blocking topology*. When using structured grid systems, two choices are possible: single-block grids and multi-block grids. Each approach has its advantages and disadvantages. For single-block grids, precise controls are needed to negotiate the series of convex and concave surfaces, while maintaining proper grid aspect ratio, orthogonality, smoothness, and grid alignment with the flow. This may require extensive internal blockings that can later be combined. One problem for single-block grids of iced airfoils that has not been resolved is illustrated in Fig. 1.⁸ In this figure, concave regions can be seen to cause grid lines to cluster, forming streaks that extend far into the flow field. These streaks can degrade the accuracy of solutions. For multi-block grids, the major problem is illustrated in Fig. 2. Grid lines that are highly clustered next to solid walls propagate into the interior of the domain along block boundaries. Since these clustered grids next to walls typically have very high aspect ratios (from hundreds to hundreds of thousands), they can induce considerable errors in the solution. If this problem is not resolved, then it is impossible to generate a high-quality multi-block structured grid for iced airfoils.

Another problem that plagues both single- and multi-block structured grids is small-scale surface jaggedness or roughness. If hyperbolic or algebraic methods are used to generate grids, then these surface discontinuities propagate into the domain interior, creating a poor quality grid.

The focus of this study is to develop methods to overcome the aforementioned problems associated with

single- and multi-block grids. All methods developed are rooted in blocking strategy, and they are presented in the next two sections.

Before presenting the methods developed in this study, it is noted that once the blocking topology has been established, many methods are available to generate high-quality grid systems. In this study, all grids were generated by using a four-boundary technique based on Hermite interpolation. This transfinite-interpolation method has controls that enable multidimensional clustering, enforce orthogonality or any other specified intersection angle at block boundaries, and ensure C^1 continuity across block boundaries.^{9,10}

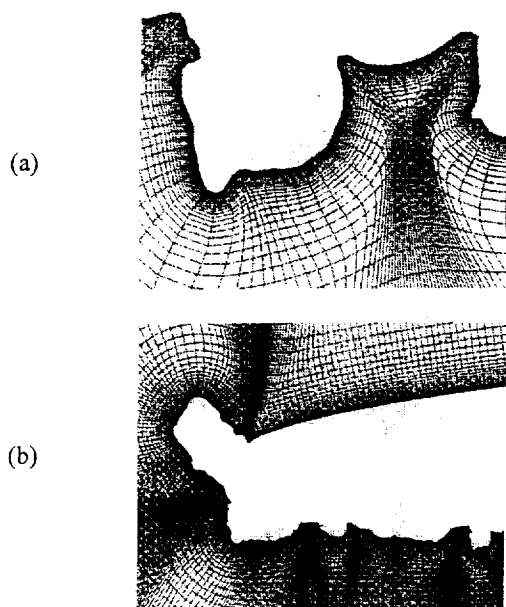


Fig. 1. Single-block grid.⁸: streaks of clustered grids extending far into the flow domain.

- (a) Close-up view showing source of streaks.
- (b) Overall view showing amount of extension.

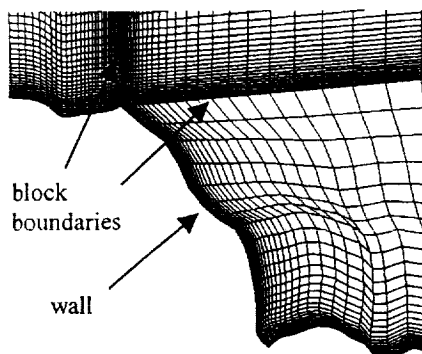


Fig. 2. Multi-block grid: grid lines clustered next to walls extend into the flow domain along block boundaries.

A METHOD FOR GENERATING HIGH-QUALITY SINGLE-BLOCK GRIDS

To illustrate the method developed in this study to overcome the problem shown in Fig. 1, consider the NLF0414 airfoil and the 623 ice shape shown in Fig. 3. The method developed involves the following three steps:

1. Generate a grid for the clean airfoil without regard for the ice shape. Since the clean airfoil is smooth, the resulting grid is smooth throughout the flow domain. A grid thus generated for the NLF0414 is shown in Fig. 4. Note that this grid is made up of two parts. One is a fine grid next to the airfoil (701×91), extending at least one chord length from the airfoil in all directions (referred to as the inner grid). The other is a coarser grid (125×21) that overlaps the fine grid by 0.1 chord length and extends at least 15 chord lengths away from the airfoil in all directions. The inner grid is the single-block grid of interest. While generating this grid, grid lines were clustered next to the airfoil surface so that the first grid point is within a y^+ of unity. Along the airfoil surface, equal arc-length concepts was employed to create as smooth a grid as possible (see Fig. 5).
2. Choose one set of grid lines near the airfoil surface, but a small distance away from the iced airfoil. All grid lines between the selected set of grid lines and the iced airfoil are regenerated to account for the accrued ice shape. Thus, the selected grid lines form two blocks. For the block that contains the iced airfoil, many sub-blocks are created in order to generate a high-quality grid. Figure 6 shows a grid generated by using this approach with the blocking topologies shown in different colors. With this blocking topology, all grids generated in all blocks can be combined into a single-block grid.
3. Repeat Step 2 until a high-quality grid is generated. This may be done in a solution-adaptive manner.

As shown in Fig. 6, the method just described can generate high quality single-block grids without streaks of highly clustered grid lines propagating into the flow domain. With this approach, only grid lines very close to the iced airfoil are affected by the ice's geometric complexities. The method just presented for iced airfoils is based on an idea proposed by Tai.¹¹

BLOCKING TOPOLOGY FOR MULTI-BLOCK GRIDS

Even though multi-block grids are generally considered to be superior to single-block grids, there are problems such as the one illustrated in Fig. 2. To further

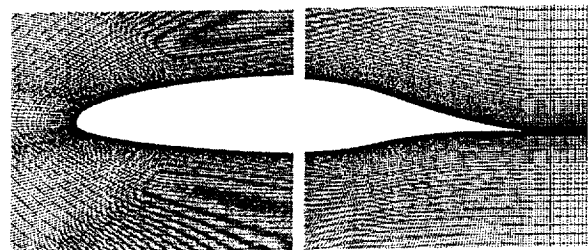
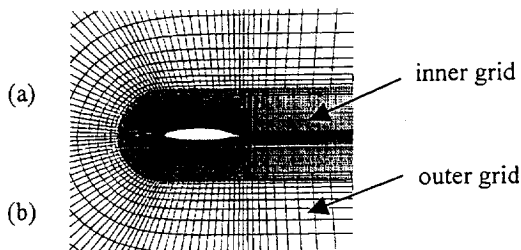
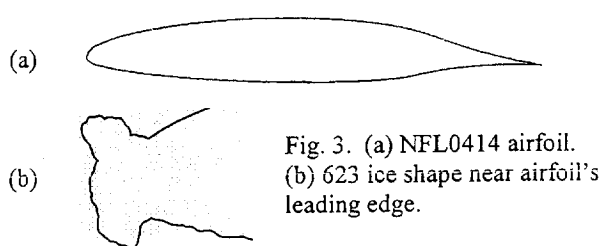


Fig. 4. Grid for clean airfoil. (a) Overall grid. (b) Inner grid near the airfoil's leading and trailing edges.

Fig. 5. Equal arc-length concept used to generate smooth grid along the airfoil.

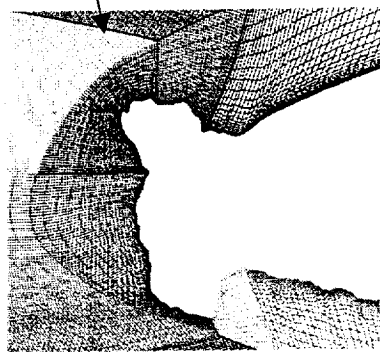


Fig. 6. Single-block grid around NFL0414 with 623 ice.

examine problems that may arise from the use of multi-block grids for iced airfoils, a multi-block grid is generated for the NLF0414 airfoil with the 623 ice. This grid is shown in Fig. 7, and two problems can be discerned. The first problem is the propagation of highly clustered grid lines into the domain interior along block boundaries, which was mentioned in relation to Fig. 2. This problem will occur whenever a block boundary next to a wall extends into the interior of the domain. The second problem shown in Fig. 7 is that roughness of ice surface propagates into the interior of the domain. This problem affects both single- and multi-block grids.

To overcome the first problem, a "thick wrap-around" grid is proposed as illustrated in Fig. 8. Basically, one layer of grid with clustering next to the wall is wrapped around the iced airfoil. The thickness of this wrap-around is such that grid spacing from contiguous blocks will be comparable in size at all block boundaries.

To overcome the second problem mentioned, a "transition-layer" grid is proposed as illustrated in Fig. 9. With a transition layer, surface discontinuities are confine

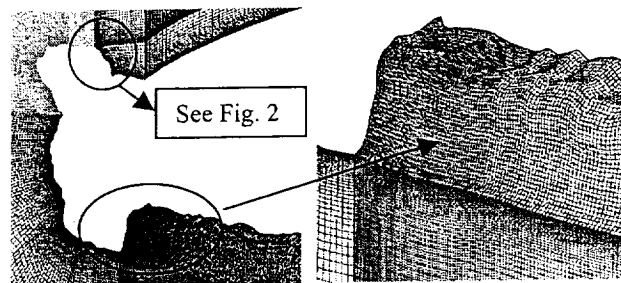


Fig. 7. A multi-block grid around NLF0414 with 623 ice.

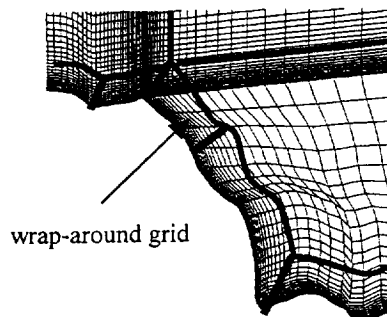


Fig. 8. "Thick wrap-around" grid.

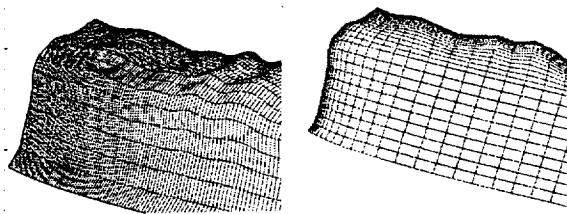


Fig. 9. "Transition-layer" grid.

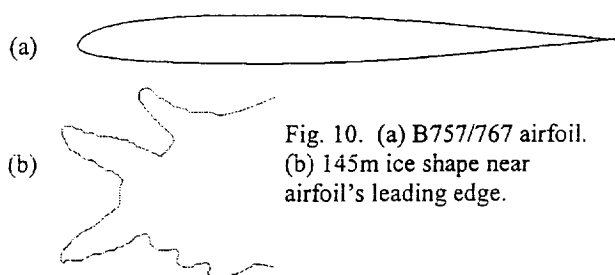


Fig. 10. (a) B757/767 airfoil.
(b) 145m ice shape near
airfoil's leading edge.

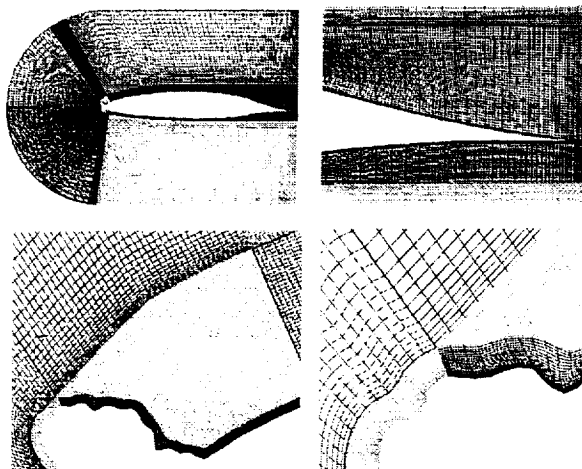


Fig. 11. A multi-block grid with "thick wrap-around"
and "transition-layer" grids for NLF0414 with 623 ice.

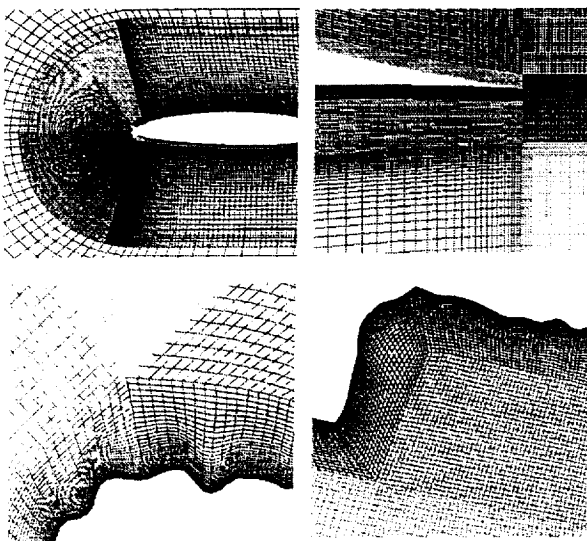


Fig. 12. A multi-block grid with a "thicker" wrap-around
grid and transition-layer grids for NLF0414 with 623 ice.

To demonstrate the usefulness of the "thick wrap-around" and the "transition-layer" grids, multi-block grids were generated for the NLF0414 airfoil with the 623 ice (Fig. 3) and the B757/767 airfoil with the 145m ice (Fig.

10). Figures 11 and 12 show two different multi-block grids for the NLF0414 airfoil with the 623 ice. They differ in the thickness of the wrap-around grid and in the block boundary near the airfoil's trailing edge. From these two figures, it can be seen that if the wrap-around grid is of the right thickness, the problem shown in Fig. 2 can be eliminated. From Fig. 12, the usefulness of the transition-layer grid is evident.

Figure 13 shows a multi-block grid for the B757/767 airfoil with the 145m ice. The high-quality grid generated for this complicated ice shape with multiple significantly protruded horns is another testament of the usefulness of the "thick wrap-around" and "transition-layer" grids.



Fig. 13. A multi-block grid with "thick wrap-around" and
"transition-layer" grids for B757/767 with 145m ice.

CFD SIMULATIONS OF FLOW OVER CLEAN AND ICED AIRFOILS

In the previous two sections, we presented two methods for generating high-quality structured grids over iced airfoils. One is a single-block grid approach for moderately complicated ice shapes. Another is a multi-block grid for highly complicated ice shapes. In this section, we show the CFD solutions generated on grid systems generated by these two methods. In the following, we first describe the flow problem, the formulation, and the flow solver. Afterwards, we present the results.

Problem Description, Formulation, and CFD Flow Solver

Two clean and two iced airfoils were simulated in order to contrast the effects of ice accretion. The two clean airfoils investigated are NLF0414 (Fig. 3) and B757/767 (Fig. 10). The two iced airfoils investigated are NLF0414 airfoil with 623 ice (Fig. 3), and B757/767 airfoil with 145m ice (Fig. 10). The detailed geometries of these airfoils and ice shapes can be found in Ref. 1. For each clean and iced airfoil, a series of angles of attack were simulated. When the angles of attack were changed, the grids were not changed.

The flow conditions employed for all simulations are as follows. The approaching Mach number is 0.29. The freestream temperature is -5°C . The Reynolds number

based on the freestream conditions and the chord length is 6.4×10^6 .

The flow past the clean and iced airfoils is model by the ensemble-averaged conservation equations of mass (continuity), momentum (full compressible Navier-Stokes), and energy for a thermally and calorically perfect gas. Turbulence is modeled by the two-equation shear-stress transport (SST) model. Wall functions were not used. Integration of the conservation equations and the SST model were to the wall, where no-slip and adiabatic wall conditions were imposed.

Though a number of open-source codes are available, one of the most versatile and well supported code is the WIND code.^{12,13} In this code, the convective terms were approximated by second-order upwind differencing formulas. Time marching to steady state was accomplished by an implicit method based on ADI-type approximate factorization.

RESULTS

A summary of all cases simulated is given in Table 1. Summarized in Table 2 is the number of grid points used for each simulation. Below, we first describe the validation of the CFD simulations. Afterwards, we examine the effects of the grids on the solutions and the convergence rate to steady state

Validation

Of the simulations performed, only the NLF0414 airfoil with and without the 623 ice have experimental data, which can be used to validate this CFD study. The experimental data is on the lift coefficient as a function of the angle of attack, and was obtained at NASA Glenn's Icing Research Tunnel and at NASA Langley's LTPT facility.¹⁴

A comparison between the CFD predicted and experimentally measured lift coefficient for the clean NLF0414 is shown in Fig. 14(a). This figure shows that CFD is able to predict the lift coefficient quite well up to and slightly past stall. After stall, however, the CFD predictions do not match the experiments. The reason for the mismatch after stall is unclear. But, the excellent agreement before stall, at stall, and slightly after stall is encouraging.

Figure 14(b) shows a comparison between the CFD predicted and experimentally measured lift coefficient for the NLF0414 airfoil with the 623 ice. In this comparison, there are two types of ice shapes in the experiments: 3D (actual 3D 623 ice shape) and 2D (i.e., same 2D ice shape for the entire airfoil span; same as CFD). The 2D ice shape selected is the one at the mid-span. From this figure, it can be seen that the agreement is good at low angles of attack. Though agreement is not as good at higher angles of attack when compared to the LTPT data, the stall angle was well predicted.

Table 1. Summary of Cases Simulated

Airfoil/Ice Shape	Grid Type*	Angle of Attack
NLF0414 / clean	SB	1.1, 6.5, 10.5, 15.6, 18.6, 20
NLF0414 / 623	SB-1	1.1, 6.2, 10.2
NLF0414 / 623	SB-2	0.0, 8.0
NLF0414 / 623	MB-1	0.0
NLF0414 / 623	MB-2	0.0, 6.0
NLF0414 / 623	MB-3	0.0
B757/767 / clean	SB	2.0, 7.0, 14.0
B757/767 / 145m	MB	0.0

* Refers to inner block (Fig. 4); SB = single block, MB = multi-block (MB-1: Fig. 7, MB-2: Fig. 11, MB-3: Fig. 12).

Table 2. Summary of Grids

Airfoil/Ice Shape	Grid Type	Grid Number*
NLF0414 / clean	SB	701 x 91
NLF0414 / 623	SB-1	781 x 70
NLF0414 / 623	SB-2	816 x 101
NLF0414 / 623	MB-1	131,197
NLF0414 / 623	MB-2	98,898
NLF0414 / 623	MB-3	111,594
B757/767 / clean	SB	977 x 101
B757/767 / 145m	MB	97,070

* Information is for inner block. The number of grid points in the outer block is 125×21 .

The comparison given above was based on CFD simulations that used in single-block grid, SB-2 (see Tables 1 and 2). The generally good agreement obtained gives some confidence to the CFD simulations performed.

Effects of Multi-Block Grids on Convergence Rate

Though "thick wrap-around" and "transition-layer" grids introduced in this study enabled the generation of high-quality multi-block grids, there is one more issue regarding the use of multi-block grids. This issue has to do with the CFD code. There are two-types of CFD codes. One type is written around the multi-block grid structure. With these codes, computations are performed in one block at a time until all blocks are computed. This process of computing in one block at a time is repeated until a converged solution is obtained on all blocks. The other type of CFD codes does not see the block boundaries when generating solutions. In those codes, each grid point or cell knows who its neighbors are, and do not use any information on the multi-block grid structure. These codes effectively see a single block grid, though they may perform domain decomposition for parallel computing.

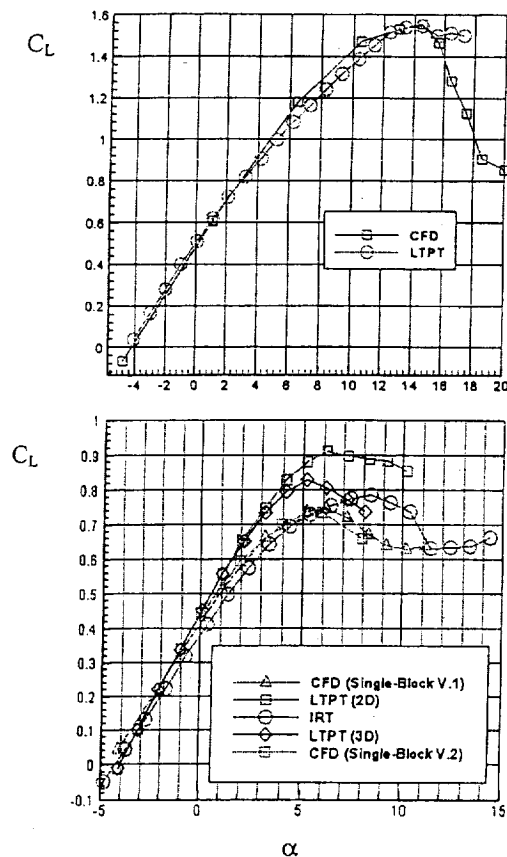


Fig. 14. Lift coefficient (C_L) as a function of attack angle (α). (a) Clean NLF0414. (b) NLF0414 with 623 ice.

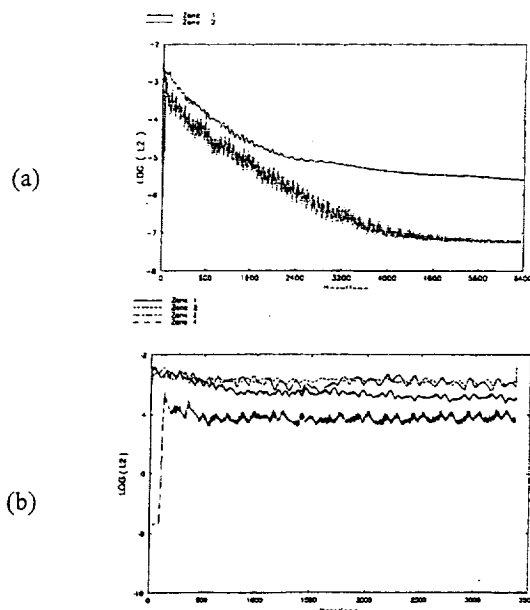


Fig. 15. Convergence history for NLF0414 with 623 ice. (a) Single-block grid (SB-2). (b) Multi-block grid (MB-3).

In this study, the WIND code is used to obtain solutions. The current version of the WIND code belongs to the first type of CFD codes mentioned. Basically, it does computations in one block at a time until all blocks are computed, and then repeats until convergence. For all of the simulations summarized in Table 1, the WIND code converged very quickly if the inner grid is a single-block grid. Figure 15(a) shows the convergence history for the case with NLF0414 airfoil, 623ice, and SB-2 grid. From this figure, it can be seen that the second norm of the residual (L2) drops more than four orders of magnitude in about 5000 iterations. Each iteration means all blocks computed once. The convergence history shown for this case is fairly typical of all single-block grids.

When the inner grid is a multi-block grid, then the convergence has been either extremely slow or do not converge as shown in Fig. 15(b). Though only a few thousand iterations are shown here, up to 30,000 iterations have been performed with the behavior being similar. The culprit is the data transfer across block boundaries in critical regions such as flow separation. Though the solutions did not converge for cases with multi-block grids, reasonable flow fields were obtained as shown below.

Flow Induced by Ice Shapes

Figure 16 shows the Mach number contours with velocity vectors in the region about the leading edge for the NLF0414 airfoil with 623 ice predicted by using SB-2 ($\alpha = 1.1$), MB-2 ($\alpha = 0$), and MB-3 ($\alpha = 0$). This comparison shows that flow features predicted are similar even though the multi-block-grid solutions did not seem to converge. From this figure, it can be seen that the two horns of the ice cause the formation of two large separated regions. Figure 17 shows the very complicated flow induced by three highly protruded horns (B757/767 with 145m ice at ($\alpha = 0$)). From this figure, it can be seen that horns, especially highly protruded ones, can severely disrupt the flow over the airfoil. Thus, it is no wonder that lift can drop so significantly and stall can occur at much lower angles of attack.

SUMMARY

A method was developed to enable the generation of high-quality single-block grids for moderately complicated ice shapes. "Thick wrap-around" and "transition layer" grids were introduced to enable the generation of high-quality multi-block grids for iced airfoils with highly complex ice shapes. For multi-block grids, the convergence issue needs to be addressed for some codes.

ACKNOWLEDGEMENT

This work was supported by NASA grant NAG 3-2576 from NASA - Glenn Research Center. The authors

are grateful for this support. The authors are also grateful to Mary B. Vickerman and Herbert W. Schilling for providing a variety of blocking topologies and helpful discussions.

REFERENCES

1. Addy, H.E., "Ice Accretions and Icing Effects for Modern Airfoils," NASA/TP-2000-210031, April 2000.
2. Chung, J.J., Choo, Y.K., Reehorst, A., Potapczuk, and Slater, J., "Navier-Stokes Analysis of the Flowfield Characteristics of an Ice Contaminated Aircraft Wing," AIAA 99-0375.
3. Chung, J.J. and Addy, H.E., "A Numerical Evaluation of Icing Effects on a Natural Laminar Flow Airfoil," AIAA Paper 2000-0096, Jan. 2000.
4. Shim, J., Chung, J., and Lee, K.D., "A Computational Investigation of Ice Geometry Effects on Airfoil Performances," AIAA Paper 2001-0540, Jan. 2001.
5. Choo, Y.K., Slater, J.W., Henderson, T., Bidwell, C., Braun, D., and Chung J.J., "User Manual for Beta Version of Turbo-GRD: A Software System for Interactive Two-Dimensional Boundary/Field Grid Generation, Modification, and Refinement," NASA TM-1998-206631, 1998.
6. Chung, J., Reehorst, A.L., Choo, Y.K., and Potapczuk, "Effects of Airfoil Ice Shape Smoothing on the aerodynamic Performance," AIAA Paper 98-3242, July 1998.
7. Vickerman, M., Choo, Y., Braun, D., Baez, M., and Gnepp, S., "SmagIce: Surface Modeling and Grid Generation for Iced Airfoils, Phase 1 Results," AIAA Paper 2000-0235, Jan. 2000.
8. Thompson, D.S. and Soni, B., "ICEG2D (v2.0) - An Integrated Software Package for Automated Prediction of Flow Fields for Single-Element Airfoils with Ice Accretion," NASA/CR-2001-210965, June 2001.
9. Shih, T.I-P., Bailey, R.T., Nguyen, H.L., and Roelke, R.J., "Algebraic Grid Generation for Complex Geometries," *International Journal for Numerical Methods in Fluids*, Vol. 13, 1991, pp. 1-31.
10. Steinthorsson, E., Shih, T.I-P., and Roelke, R.J., "Enhancing Control of Grid Distribution in Algebraic Grid Generation," *International Journal for Numerical Methods in Fluids*, Vol. 15, 1992, pp. 297-311.
11. Tai, T.C., "Single-Block Structured Body-Conforming Grid for Complex Geometries," *Numerical Grid Generation in Computational Field Simulations*, edited by B.K. Soni, J.F. Thompson, J. Hauser, and P. R. Eiseman, ISGG, Mississippi State University, 2000, pp. 91-100.
12. Power, G.D. and Underwood, M.L., "WIND 2.0: Progress on an Applications-Oriented CFD Code," AIAA Paper 99-3212, June 1999.
13. Michal, T. and Oser, M., "Improving Zonal Coupling Accuracy and Robustness in the WIND Code," AIAA Paper 2001-0222, Jan. 2001.
14. Addy, H., Chung, J., "A Wind Tunnel Study of Icing on a Naturally Laminar Flow Airfoil," AIAA Paper 2000-0095, January 2000

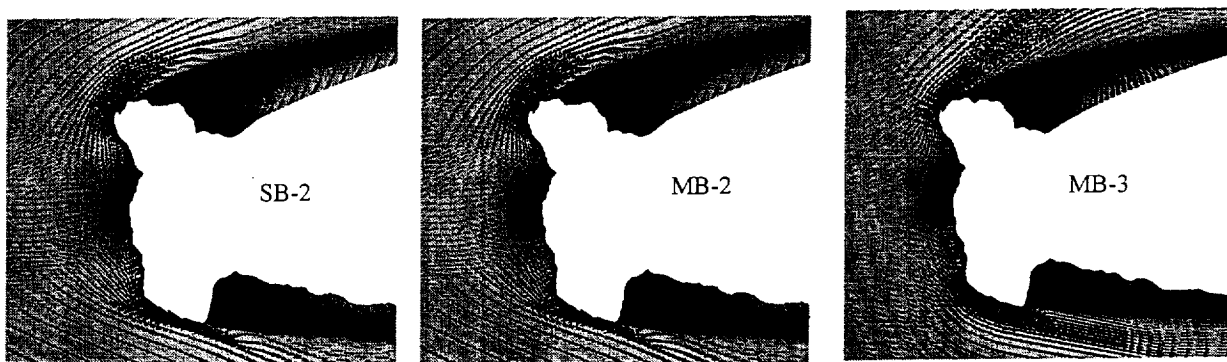


Fig. 16. Predicted Mach number and velocity vectors near the leading edge of NLF0414 with 623 ice.

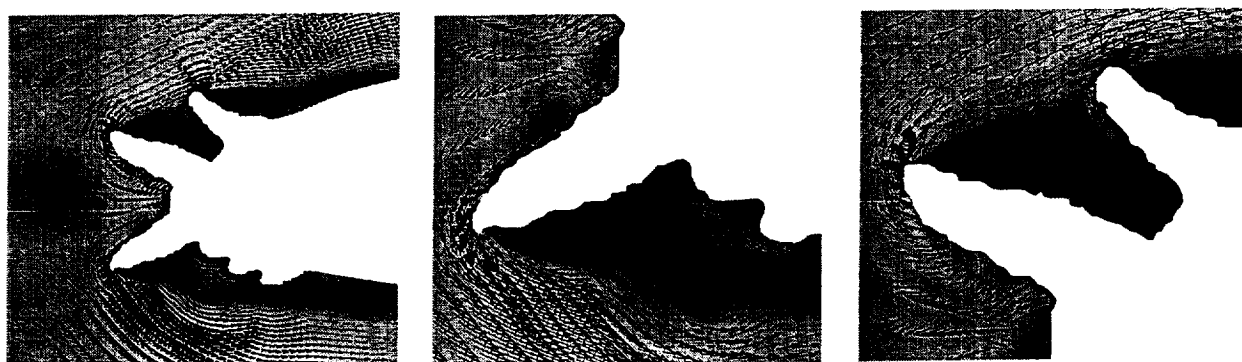


Fig. 17. Predicted Mach number and velocity vectors near the leading edge of B757/767 with 145m ice.

